12 Superconductivity and Magnetism

M. Angst (since December 2002), M. Bruun (since November 2002), D. Di Castro, D.G. Eshchenko (since April 2002), H. Keller, R. Khasanov, S. Kohout M. Mali, J. Roos, A. Shengelaya
M. Eremin (visiting scientist), V.A. Ivanshin (visiting scientist), B. Kochelaev (visiting scientist)
T. Schneider (Titularprofessor), and K.A. Müller (Honorarprofessor)

in collaboration with:
ETH Zürich (K. Conder, J. Karpinski), Paul Scherrer Institute (E. Morenzoni), IBM Rüschlikon Research Laboratory (J.G. Bednorz), University of Birmingham (E.M. Forgan), University of St. Andrews (S.L. Lee), University of Rome (A. Bianconi), Kazan State University (A. Dooglav, M.V. Eremin, B.I. Kochelaev), University of Belgrade (I.M. Savić), Institute of Low Temperature and Structure Research, Polish Academy of Sciences, Wroclaw (P.W. Klamut), Institute of Physics, Polish Academy of Sciences, Warsaw (R. Puzniak, A. Wisniewski), University of Tokyo (K. Kishio, T. Sasagawa, H. Takagi), Northern Illinois University, DeKalb (B. Dabrowski).

In the last year we continued our investigations on the fundamental physical properties of non-conventional superconductors (hole and electron doped cuprates and magnesium diboride). A great advantage of our approach is the combined application of complementary experimental techniques, such as muon-spin rotation (μSR), nuclear magnetic resonance (NMR), nuclear quadrupole resonance (NQR), electron paramagnetic resonance (EPR), together with bulk SQUID and torque magnetometry and resistivity, to investigate these systems. One of our main research interests concerns detailed oxygen isotope (^{16}O/^{18}O) effect (OIE) studies on various physical quantities and phenomena (critical temperature, in-plane penetration depth, charge fluctuations) in cuprate high-temperature superconductors (HTSC) in order to explore the role of the electron-phonon interaction in the basic physics of these systems. In another project, we investigated for the first time the magnetic penetration depth in an electron doped infinite layer HTSC ($Sr_{0.9}La_{0.1}CuO_2$) by μSR. Furthermore, we continued the magnetic torque studies of single-crystal magnesium diboride (MgB_2) to clarify the peculiar magnetic properties of this novel two-band superconductor. In addition, we performed a preliminary boron isotope (^{10}B/^{11}B) effect (BIE) study of the magnetic penetration depth in MgB_2 using μSR. The scientific goal of our research is to get a better understanding of the basic physical processes involved in HTSC, MgB_2 and related novel superconductors.

12.1 Studies of oxygen isotope effects in cuprates

12.1.1 Direct observation of the oxygen isotope effect on the magnetic field penetration depth in optimally doped $YBa_2Cu_3O_{7-\delta}$

There is increasing evidence that strong lattice effects are present in HTSC, which may lead to the formation of polarons (bare charge carriers accompanied by local lattice distortions) [1; 2]. One way to test this hypothesis is to demonstrate that the effective mass of the supercarriers m^* depends on the mass M of the lattice atoms. This is in contrast to conventional BCS superconductors, where m^* is independent of M. For HTSC (clean limit) the in-plane penetration depth λ_{ab} obeys the relation $\lambda_{ab}^{-2}(0) \propto n_s/m_{ab}^*$, where n_s is the superconducting charge carrier density, and m_{ab}^* is the in-plane effective mass of the supercarriers. This implies that the OIE on $\lambda_{ab}(0)$ is due to a shift in n_s and/or

m^*_{ab}, according to the relation:

$$\Delta\lambda_{ab}(0)/\lambda_{ab}(0) = 1/2\ [\Delta m^*_{ab}/m^*_{ab} - \Delta n_s/n_s]. \qquad (12.5)$$

Therefore a possible mass dependence of m^*_{ab} can be tested by investigating the isotope effect on λ_{ab}, provided that the contribution of n_s to the total isotope shift is known. Over recent years we performed detailed investigations of the OIE on $\lambda_{ab}(0)$ in underdoped $La_{2-x}Sr_xCuO_4$ by means of magnetization [3; 4] and torque magnetometry [5], as well as in underdoped $Y_{1-x}Pr_xBa_2Cu_3O_{7-\delta}$ by means of μSR [6]. As result, we found a remarkable relative isotope shift of $\Delta\lambda^{-2}_{ab}(0)/\lambda^{-2}_{ab}(0)$ of -5 to -10% in these cuprate systems.

Recently, we were able to observe a substantial OIE on $\lambda_{ab}(0)$ in an optimally doped $YBa_2Cu_3O_{7-\delta}$ film by using the novel low-energy μSR technique (LEμSR), developed at the Paul Scherrer Institute (PSI) [7]. In a LEμSR experiment slow spin-polarized muons of tunable energy between 0 and 30 keV are implanted at very small and controllable depth below the surface of a sample. This peculiarity allows to exploit all the advantages of bulk μSR in studies of local magnetic fields in thin samples, near surfaces, and as a function of depth below surfaces. Due to the random nature of the muon scattering process, LE muons do not stop at a sharp depth below the surface of the sample. The implantation depths are distributed over a nanometer scale, and the implantation depth profile $n(z)$ depends on the muon energy. This feature offers a unique possibility to measure the internal magnetic field profile $B(z)$ over some interval of distances z below the surface of a superconducting sample for a given muon energy. This so-called integral reconstruction (IR) method was recently developed by A. Suter [10]. The IR method is based on a simple approximation that links the magnetic field probability distribution $p(B)$ to the muon implantation depth distribution $n(z)$ [10]:

$$n(z)dz = p(B)dB. \qquad (12.6)$$

Integration of both sides of Eq.(12.6) gives:

$$\int_z^\infty n(\zeta)d\zeta = \int_0^{B(z)} p(\beta)d\beta, \qquad (12.7)$$

where $n(\zeta)$ is emulated and $p(\beta)$ is determined experimentally. For any given z Eq.(12.7) can be solved numerically, and the appropriate magnetic field profile $B(z)$ can be reconstructed (see Fig. 12.1).

The big advantage of the IR method in comparison with the previously used mean-value approx-

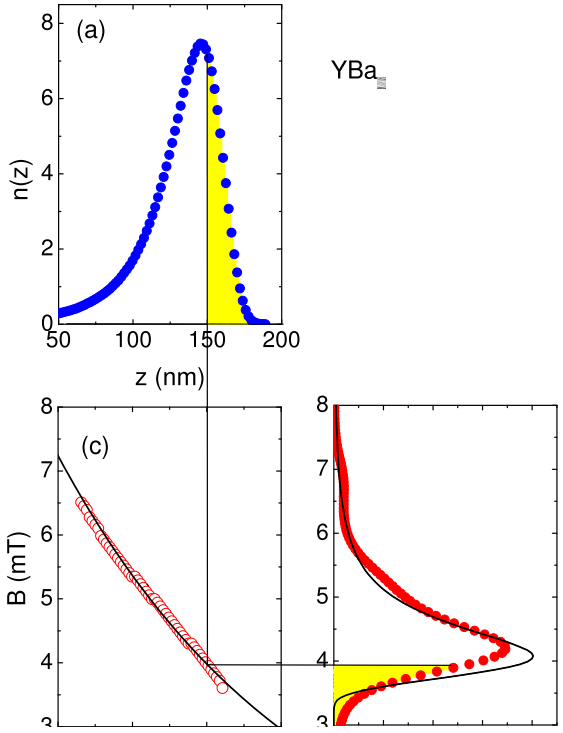

Figure 12.1: *Principle of the integral reconstruction method. (a) Calculated muon implantation depth distribution $n(z)$ using the Monte-Carlo code TRIM.SP [8]. (b) Measured probability field distribution $p(B)$ in the Meissner state, obtained from the μSR time domain spectrum by the Maximum Entropy Fourier method [9]. (c) Reconstructed field profile $B(z)$. Filled areas in (a) and (b) are equal, giving the integral equation for $B(z)$. Solid line in (c) is the best fit of Eq.(12.8) to the reconstructed $B(z)$. Solid line in (b) represents the field distribution $p(B)$ calculated for the best fit in (c) and $n(z)$ in (a).*

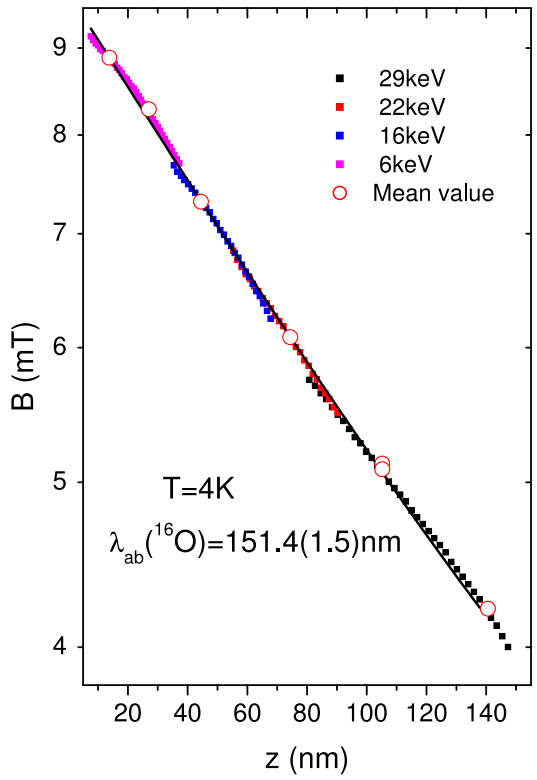

Figure 12.2: *Reconstructed magnetic field profile $B(z)$ for the ^{16}O substituted $YBa_2Cu_3O_{7-\delta}$ film measured at 4 K in the Meissner state in a magnetic field of 9.2 mT applied parallel to the surface of the film. The integral reconstruction is shown for the muon implantation energies 29, 22, 16, and 6 keV. The mean-value reconstruction is shown for implantation energies 29, 22, 16, and 6 keV (open circles). The solid curve represents the best fit by Eq.(12.8).*

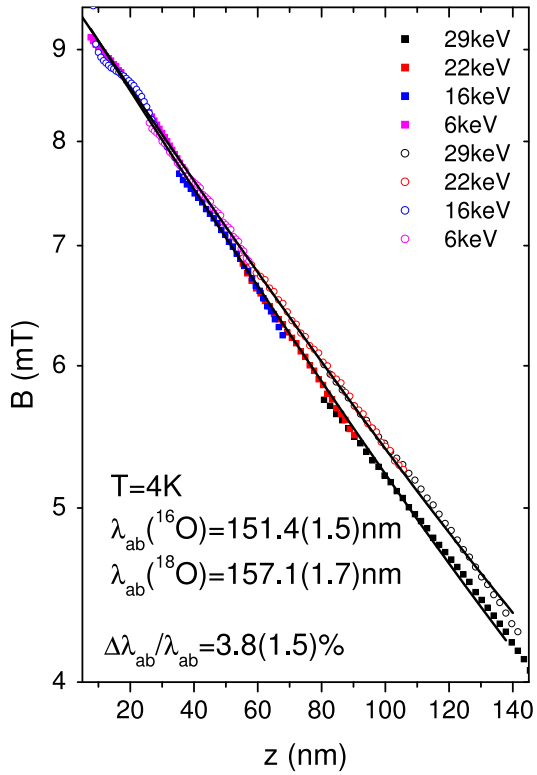

Figure 12.3: *Magnetic penetration profile of the $^{16}O/^{18}O$ substituted $YBa_2Cu_3O_{7-\delta}$ films in the Meissner state at various muon implantation energies (29, 22, 16, and 6 keV). The solid curves are fits according to Eq.(12.8).*

imation (MVA) [11] is obvious. Both methods use emulated $n(z, E)$ and a sequence of experimental μSR spectra measured at different implantation energies E. In the MVA only one point $B(z_E)$ (where z_E is the mean implantation depth for a given E) is extracted per spectrum, while in the IR method $B(z)$ can be reconstructed over a relatively wide interval of z.

We used the advantages of the IR method for the direct measurement of the oxygen isotope ($^{16}O/^{18}O$) effect on the in-plane penetration depth in an optimally doped $YBa_2Cu_3O_{7-\delta}$ film. The experiments were performed on a 600 nm thick epitaxial $YBa_2Cu_3O_{7-\delta}$ film in the Meissner state. A weak external magnetic field of 9.2 mT was applied parallel to the surface and perpendicular to the c-axis of the sample. The field profile $B(z)$ was reconstructed by the IR method for several implantation energies (from 3 to 30 keV), corresponding to implantation depths in the range 15-150 nm. The experimental field profile (Fig. 12.2) is in excellent agreement with the London theory for a slab of thickness $2t$ in the Meissner state:

$$B(z) = B_0 \frac{\cosh[(t-z)/\lambda_{ab}]}{\cosh(t/\lambda_{ab})}. \tag{12.8}$$

For the ^{16}O substituted $YBa_2Cu_3O_{7-\delta}$ film a fit of Eq.(12.8) to the reconstructed $B(z)$ yields $^{16}\lambda_{ab}(4K) = 151.4(1.5)$ nm. Note the accuracy of the IR method – the absolute value of λ_{ab} can be measured with a precision better than 1%. This means that an OIE on λ_{ab} of 1.4% or larger can easily be detected by LEμSR. Fig. 12.3 shows the field profiles determined by the IR method for $YBa_2Cu_3O_{7-\delta}$ films with two different oxygen isotopes ^{16}O and ^{18}O. It is seen that the data points for the ^{18}O sample are systematically higher than those for the ^{16}O sample, indicating that $^{16}\lambda_{ab} < {}^{18}\lambda_{ab}$. A fit with Eq.(12.8) gives $^{18}\lambda_{ab} = 157.1(1.7)$ nm. The relative oxygen isotope shift of the in-plane penetration depth was found to be $\Delta\lambda_{ab}/\lambda_{ab} = 3.8(1.5)\%$.

It was shown [3; 4; 5; 6] that the OIE on λ_{ab} arises mainly from the oxygen-mass dependence of the in-plane effective mass m^*_{ab}. The present result indicates that lattice effects even at optimal doping play an essential role in cuprate superconductors.

[1] A.S. Alexandrov and N.F. Mott, Int. J. Mod. Phys. **8**, 2075 (1994).

[2] K.A. Müller, Physica C **341-348**, 11 (2000).

[3] G.M. Zhao *et al.*, Nature (London) **385**, 236 (1997).

[4] G.M. Zhao *et al.*, J. Phys.: Condens. Matter **10**, 9055 (1998).

[5] J. Hofer *et al.*, Phys.Rev.Lett.**84**, 4192 (2000).

[6] R. Khasanov *et al.*, J. Phys. : Condens. Matter **15**, L17 (2003).

[7] E. Morenzoni *et al.*, J. Appl. Phys. **81** 3340 (1997).

[8] B.D. Rainford and G.J. Daniel, Hyperfine Interact. **87** 1129 (1994).

[9] W. Eckstein, *Computer Simulations of Ion-Solid Interactions*(Springer-Verlag, Berlin, 1992).

[10] A. Suter *et al.*, unpuplished.

[11] T.J. Jackson *et al.*, Phys. Rev. Lett. **84**, 4958 (2000).

12.1.2 Oxygen isotope effect on charge fluctuations observed by NQR at very low temperatures in $YBa_2Cu_4O_8$

It is our anticipation that knowledge of the OIE on different NMR/NQR parameters measured at plane-copper as well as at yttrium sites in $YBa_2Cu_4O_8$ will add clues to the understanding of high-T_c superconductivity. The major part of the copper hyperfine Hamiltonian comes from the interactions of the nuclear spin with its electronic environment. These hyperfine interactions are responsible for the Knight shift, the spin-lattice relaxation rate, and the unusual temperature dependence of the NQR line frequency and its linewidth [1]. Having different copper isotopes we are able to distinguish between two kinds of hyperfine interactions: the magnetic one caused by the electron spin and the quadrupolar (electric) one caused by the electron charge. This differentiation is possible because the magnetic interactions depend on the nuclear magnetic dipole moment and the quadrupolar ones on the nuclear electric quadrupole moment.

In normal conducting $YBa_2Cu_4O_8$ the plane-copper spin-lattice relaxation is predominantly of magnetic origin caused by spin fluctuations and its temperature dependence is controlled by the spin-pseudogap phenomenon [2]. In the superconducting phase this magnetic contribution to the relaxation diminishes due to the d-wave superconducting gap.

Our recent NQR measurements of the ^{63}Cu and ^{65}Cu relaxation rates in superconducting $YBa_2Cu_4O_8$ show that the reduced spin-lattice relaxation gradually changes its character by becoming progressively more quadrupolar due to yet unidentified low frequency charge fluctuations [3]. At very low

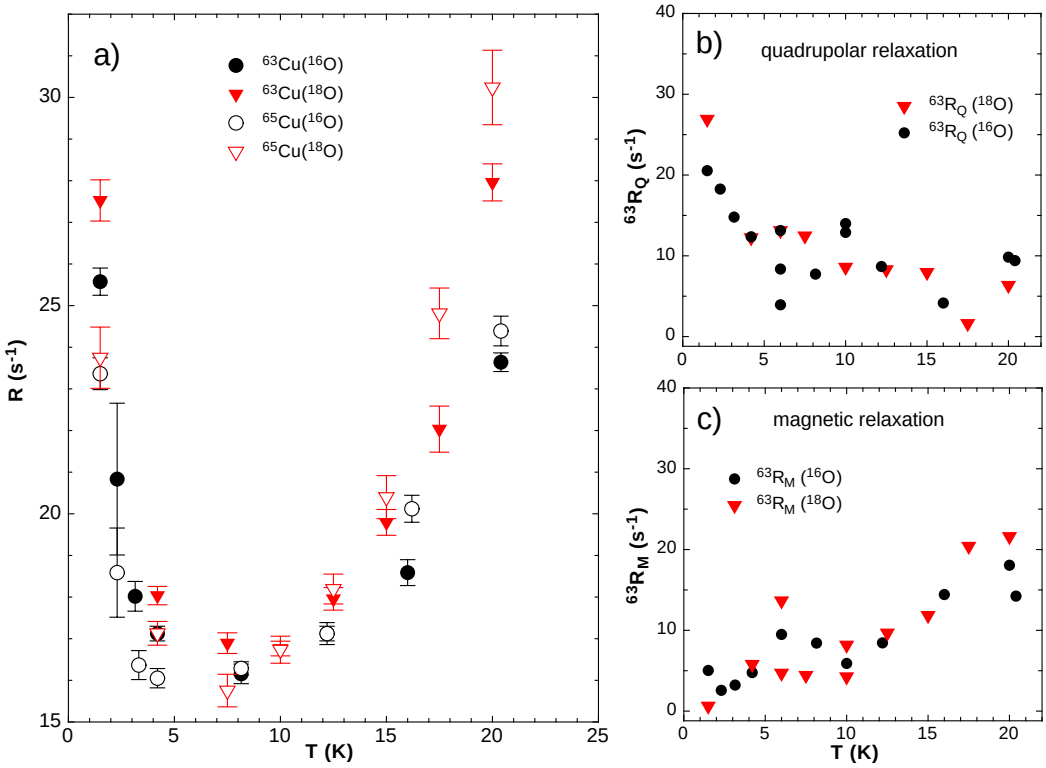

Figure 12.4: *Temperature dependence of: a) plane-^{65}Cu and ^{63}Cu spin-lattice relaxation rate R in superconducting ^{16}O and ^{18}O $YBa_2Cu_4O_8$, b) quadrupolar contribution, R_Q, and c) magnetic contribution, R_M, to R in superconducting ^{16}O and ^{18}O $YBa_2Cu_4O_8$.*

temperature the relaxation gets predominantly quadrupolar with an unexpected temperature dependence. The quadrupolar rate instead to reduce with decreasing temperature has the tendency to grow. In Figure 12.4 a) we present ^{63}Cu and ^{65}Cu relaxation rates R for ^{16}O and ^{18}O $YBa_2Cu_4O_8$ below 20 K. By inspection one notices that there is an OIE since $^{65,63}R(^{18}O)$ is always larger than the corresponding $^{65,63}R(^{16}O)$. This means that the low frequency spectral density of fluctuations at the NQR frequency is higher in the ^{18}O superconductor than in the ^{16}O superconductor. In Fig. 12.4 b) and 12.4 c) we present separately the quadrupolar (R_Q) and magnetic (R_M) contributions to ^{63}R for ^{16}O and ^{18}O exchanged $YBa_2Cu_4O_8$. One notices that for both oxygen isotopes R_M diminishes whereas R_Q grows with decreasing temperature. The separation procedure inevitably enhances the scatter of the results, so a separate OIE determination of R_M and R_Q is not possible. The completely opposite temperature behavior of R_Q and R_M is striking. While the known spin fluctuations die out, new low frequency charge fluctuations develop, which show no tendency to abate at 1.5 K, the lowest temperature we measured. The quasi particles responsible for these new charge excitations have no spin and live in the superconducting phase at 1 K and below. The question arises which type of quasiparticles this could be. At the moment we are still missing an adequate explanation for the observed quadrupolar contribution to the relaxation.

[1] M. Mali *et al.*, Phys.Rev.B **65**, 184518 (2002).

[2] F. Raffa *et al.*, Phys.Rev.Lett.**81**, 5912 (1998); M. Bankay *et al.*, Phys.Rev. B **50**, 6416 (1994).

[3] M. Mali *et al.*, Journal of Superconductivity: Incorporating Novel Magnetism **15**, 511 (2002).

12.2 μSR studies of electron-doped $Sr_{0.9}La_{0.1}CuO_2$

The high-T_c cuprate superconductors are obtained by doping holes or electrons into the antiferromagnetic (AF) insulating state. Both electron and hole-doped cuprates share a common building block, namely the copper-oxygen plane. Therefore, one would expect that the same pairing mechanism applies in both cuprate superconductors. In order to elucidate the mechanism of high-T_c superconductivity, it is very important to clarify the origin of the similarities and the differences between the hole-doped (p-type) and the electron-doped (n-type) cuprates.

The magnetic field penetration depth λ is one of the fundamental lengths of a superconductor. Detailed μSR investigations of polycrystalline cuprate superconductors have demonstrated that λ can be obtained from the muon spin depolarization rate $\sigma(T) \sim 1/\lambda^2(T)$ [1]. In contrast to p-type cuprates there is no consensus about the penetration depth value for n-type cuprates. Problems concerning the sample quality and the large dynamic relaxation due to rare-earth magnetic moments in n-type cuprates $R_{2-x}Ce_xCuO_{4-\delta}$ (R= Nd, Sm, Pr) with so-called T'-structure prevented the determination of $\sigma(0)$ using μSR [2].

There exists another class of n-type cuprates (Sr,Ln)CuO_2 (Ln=La, Sm, Nd, Gd) with the so-called infinite-layer structure (ILS). The n-type ILS superconductors have several merits. First, they have the simplest crystal structure among all HTSC consisting of an infinite stacking of CuO_2 planes and (Sr, Ln) layers. The charge reservoir block of the rock-salt type or fluorite type in HTSC does not exist in the infinite-layer structure. Second, their oxygen content is stoichiometric without vacancies or interstitial oxygen. Third, n-type ILS have much higher T_c ($\simeq$ 43 K) compared to the n-type cuprates with T'-structure ($T_c \simeq$ 25 K). Recently, we studied the penetration depth in high-quality $Sr_{0.9}La_{0.1}CuO_2$ ILS using the transverse-field (TF) μSR technique. Fig. 12.5 shows the temperature dependence of the TF-μSR depolarization rate σ at B_{ext}=0.6 T.

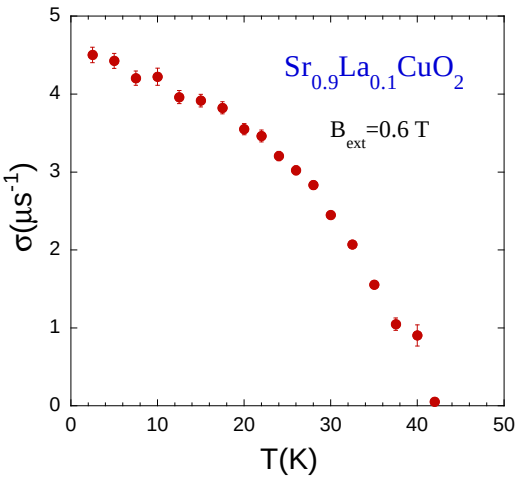

Figure 12.5: *Temperature dependence of the μSR depolarization rate σ of $Sr_{0.9}La_{0.1}CuO_2$.*

We confirmed microscopically that this compound is a bulk superconductor. Because of the absence of magnetic rare-earth ions, it was possible to measure the penetration depth in a n-type HTSC for the first time using μSR. We obtained the value $\lambda_{ab}(0)$=1170(12) Å . The zero-temperature depolarization rate $\sigma(0)$=4.6(1) μs^{-1} is more than four times larger than expected from the Uemura plot. This shows that the n-type ILS does not follow the Uemura relation established in p-type HTSC [3].

[1] See, e.g. H. Keller, in *Materials and Crystallographic Aspects of HTc-Superconductivity*, edited by E. Kaldis (Kluwer Academic Publishers, 1994), p.265; J.E. Sonier *et al.*, Rev. Mod. Phys. **72**, 769 (2000).

[2] G.M. Luke *et al.*, Phys.Rev.B **42**, 7981 (1990).

[3] Y.J. Uemura *et al.*, Phys.Rev.Lett.**62**, 2317 (1989).

12.3 Studies of magnesium diboride

12.3.1 μSR investigations of Boron isotope effect

Soon after the discovery of the novel superconductor MgB_2 [1] the isotope shift on T_c was investigated in detail [2; 3]. Whereas the boron-isotope ($^{10}B/^{11}B$) exponent was found to be $\alpha_B \simeq 0.28(2)$ [2; 3], only a small magnesium-isotope ($^{24}Mg/^{26}Mg$) effect with $\alpha_{Mg} \simeq 0.02(1)$ [3] was detected. It is interesting to note that in this layered superconductor the predominant contribution to the total isotope shift on T_c arises from the B atoms in the planes where superconductivity takes place, similar to the layered cuprate HTSC [4; 5]. In the latter a substantial shift on the magnetic penetration depth λ under oxygen isotope substitution was observed [3; 4; 5; 6], indicating that lattice effects play an important role in these systems.Therefore, we recently performed a detailed study of the boron isotope effect on the magnetic penetration depth in MgB_2 in order to clarify the role of the electron-phonon interaction in this compound. The μSR technique was used to explore the local magnetic field distribution $p(B)$ in the mixed state of polycrystalline MgB_2. The muon spin depolarization rate σ, which under certain conditions (see below) is proportional to the second moment of $p(B)$, is a direct measure of the magnetic penetration depth λ. The muon spin-depolarization rate was studied as a function of temperature and magnetic field. The results for the natural abundant boron sample MgB_2 are in good agreement with previous μSR results [6; 7]. Here we report the μSR results on $Mg^{11}B_2$ and $Mg^{10}B_2$ samples. In Fig. 12.6 the low-temperature field dependence of σ for the $Mg^{11}B_2$ sample indicates the presence of pinning induced distortion of the vortex lattice at low magnetic fields. At higher fields ($B \geq 0.4$ T) σ was found to be nearly field independent, as expected for an ideal vortex lattice. Only in this case σ is a direct measure of the magnetic penetration depth λ.

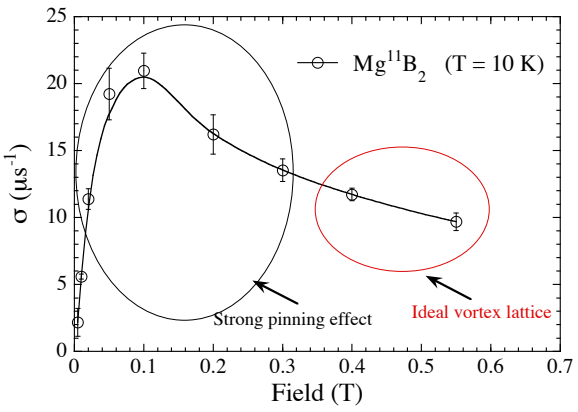

Figure 12.6: *Magnetic field dependence of the muon-spin depolarization rate σ for $Mg^{11}B_2$. The regions with strong and weak pinning induced distortion of the vortex lattice are indicated with black and red circles, respectively.*

The temperature dependence of σ for the $Mg^{10}B_2$ and $Mg^{11}B_2$ samples, measured at high fields (B = 0.4 T), reflecting $\lambda^{-2}(T)$, is shown in Fig. 12.7. A clear shift in T_c of ΔT_c = 0.9(1)K is visible , in agreement with previous results [2; 3]. However, at low temperature the two curves merge. The μSR data were fitted to the two gap equation [6], yielding the following $\sigma(0)$ values of the two isotope samples: $\sigma(0)^{^{10}B}$=13.26(14)μs^{-1} and $\sigma(0)^{^{11}B}$=13.18(27)μs^{-1}. The relative isotope shift is very small with a rather large relative error: $\Delta\sigma(0)/\sigma(0) = -0.6(2.2)\%$. From this result we estimate the upper limit of the boron isotope effect on the magnetic penetration depth to be

$$\mid \Delta\sigma(0)/\sigma(0) \mid = \mid \Delta\lambda^{-2}(0)/\lambda^{-2}(0) \mid < 3\%. \tag{12.9}$$

Considering that MgB_2 is close to the clean limit [8; 9; 10], the relation $\lambda_{ab}^{-2}(0) \propto n_s/m^*$ holds, where n_s and m^* denote the density and effective mass of the superconducting charge carriers, respectively. According to Eq.(12.5) an isotope shift on λ_{ab} then should be due to a shift in n_s and/or m^*. We can assume that the isotope substitution does not affect the superfluid density, for the fol-

lowing reasons: (i) With changing the isotope we are changing only the mass of the nuclei, and not directly the charge carrier density. (ii) The x-ray diffraction measurements, performed before the μSR experiments, showed that within experimental error, there is no difference in the lattice parameters between the two isotope samples. So, there are at least no changes in the conducting bands due to structural modifications. Thus we can conclude that Eq.(12.9) sets an upper limit for a possible isotope effect on the charge carrier effective mass in MgB_2. This conclusion may be interpreted as a confirmation for MgB_2 to be a conventional phonon-mediated superconductor. However, further theoretical calculations are needed in order to estimate what kind of contribution to the total isotope effect may arise from each one of the two effective masses in a two-gap superconductor such as MgB_2.

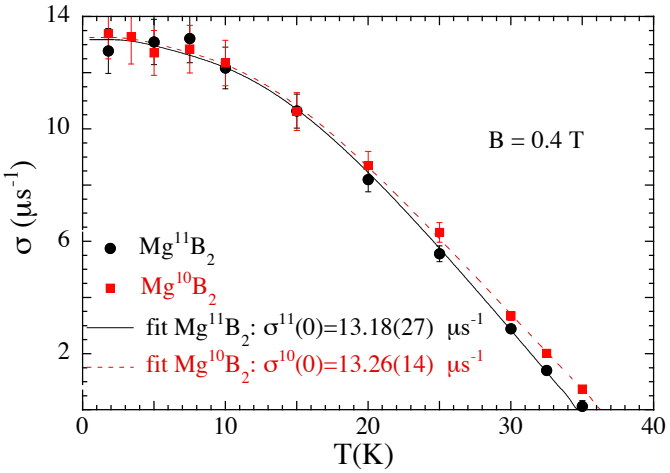

Figure 12.7: *Temperature dependence of the muon-spin depolarization rate for the two Boron isotope substituted MgB_2 samples. A clear shift of the two curves is present close to T_c, but at low temperatures they merge together.*

[1] J. Nagamatsu *et al.*, Nature (London) **410**, 63 (2001).
[2] S. L. Bud'ko *et al.*, Phys.Rev.Lett.**86**, 1877 (2001).
[3] D. G. Hinks *et al.*, Nature **411**, 457 (2001).
[4] D. Zech *et al.*, Nature (London) **371**, 681 (1994).
[5] G.M. Zhao *et al.*, J. Phys.: Condens. Matter **13**, R569 (2001).
[6] Ch. Niedermayer *et al.*, Phys.Rev.B **65**, 094512 (2002).
[7] K. Ohishi *et al.*, J. Phys. Soc. Jpn. **72**, 29 (2003).
[8] A. V. Sologubenko *et al.*, Phys.Rev.B. **65**, 180505 (2002).
[9] F. Bouquet *et al.*, Phys.Rev.Lett.**89**, 257001 (2002).
[10] A. V. Sologubenko *et al.*, Phys.Rev.B. **66**, 014504 (2002).

12.3.2 Magnetometry measurements

The anisotropic Ginzburg-Landau theory (AGLT) is very successful in describing most of the magnetic properties of the cuprate superconductors. However, for MgB_2 various deviations were observed. A refinement of the AGLT is needed, because MgB_2 is a two-gap-superconductor. We compared our torque magnetometry results with recent theoretical predictions of deviations from the AGLT.

In a torque experiment a single crystal is exposed to an external magnetic field, and the mechanical torque it experiences is measured (see section 12.4.1) as a function of time, temperature, magnetic field strength, and the angle enclosed by the field and a characteristic sample direction. Figure 12.8 shows an angle dependent measurement. It was suggested that the anisotropy (i.e. the ratio of a quantity along two perpendicular directions) of the two main superconducting properties – the penetration depth λ and the coherence length ξ (resp. the upper critical field H_{c2}) – might be different in two-gap-superconductors such as MgB_2. Based on this, Kogan [1] predicted a sign change of the torque for low temperatures. The dashed line in Fig. 12.8 illustrates this sign change for field directions close to the boron layers ($\theta = 90°$). Such a feature is not visible in the experimental data (Fig. 12.8). This discrepancy suggests that the difference between the two anisotropies cannot be as large as currently assumed. The theory might be reconciled with our results by working out explicitly the influence of the magnetic field strength on the anisotropy.

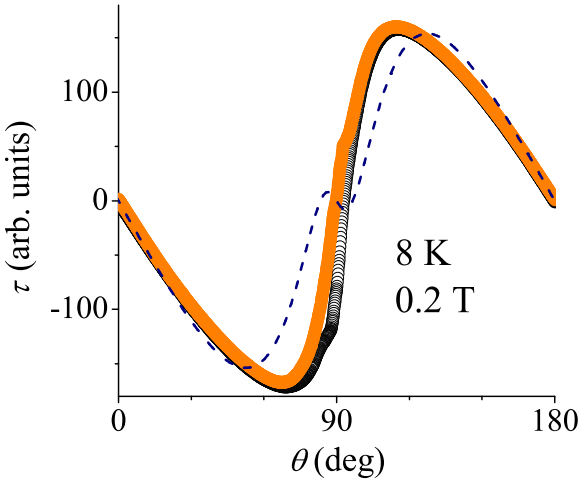

Figure 12.8: *Angle dependent torque measurement at low temperature in a low magnetic field.*

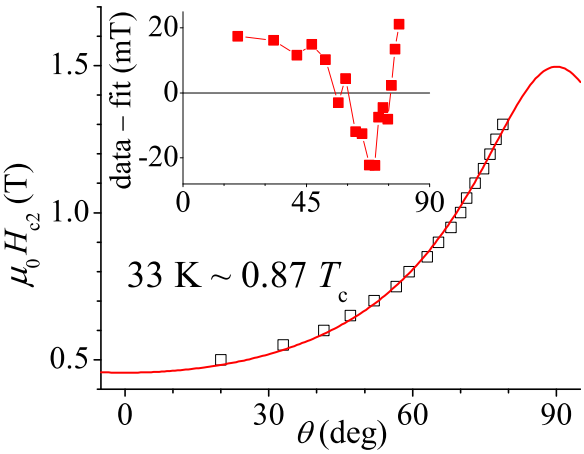

Figure 12.9: *Measured $H_{c2}(\theta)$ and a best fit of the AGLT to the data. The inset shows the difference between the data and the fit.*

A different deviation from the AGLT occurs in the angle dependence of the upper critical field $H_{c2}(\theta)$ (see Fig. 12.9). These systematic deviations can be very well approached by the recent theoretical work of Golubov and Koshelev [2]. Both the shape and the magnitude of the calculated deviations look very similar to our data.

[1] V. G. Kogan, Phys.Rev.Lett.**89**, 237005 (2002).

[2] A. A. Golubov and E. A. Koshelev, cond-mat/0303237.

12.4 New developments in instrumentation

12.4.1 Micro-torque sensors

Torque magnetometry is an excellent tool for performing highly sensitive measurements of magnetic properties of anisotropic superconductors, such as the cuprates or magnesium diboride. In a torque experiment a sample is mounted on an appropriate cantilever. By applying an external magnetic field, the sample experiences a torque which causes the sensor to be deflected in a characteristic way.

We are using two different readout schemes to measure this deflection. In the capacitive technique a capacitance change, caused by the displacement of a flexible electrode, is measured. In the piezoresistive technique, on the other hand, specifically formed piezoresistors are fabricated on the bending structures of the sensor. The stress caused by a torque changes their resistance. Careful placement of the electrodes and the readout leads of a capacitive torque sensor (see Fig. 12.10) allowed us to reach sensitivities comparable to those reported for the much more expensive piezoresistive sensors. The piezoresistive torque sensors developed by our group [1; 2; 3] have noise levels of the order of 10^{-14} Nm, whereas test measurements using the new capacitive torque sensor with a piece of magnetic tape had standard deviations of the torque as low as $3 \cdot 10^{-14}$ Nm. In an attempt to further increase the sensitivity of the piezoresistive technique, a new design of sensors was recently developed, shown in figure 12.11. Unfortunately, due to delays in the fabrication of the sensors, no results can be reported so far. But elasticity calculations suggest that the sensitivity is increased by a factor of about 2 compared to the previous devices [1; 2; 3]. This geometry allows for a choice of sensitivity by tuning the leg length l and the platform width b (a larger ratio l/b results in a higher sensitivity).

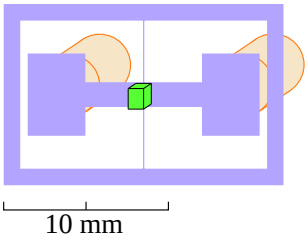

Figure 12.10: *Schematic of a capacitive torque sensor with a mounted sample (green cube). The capacitance difference between the active (purple) and the two excitation electrodes (orange) is measured.*

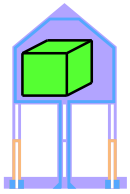

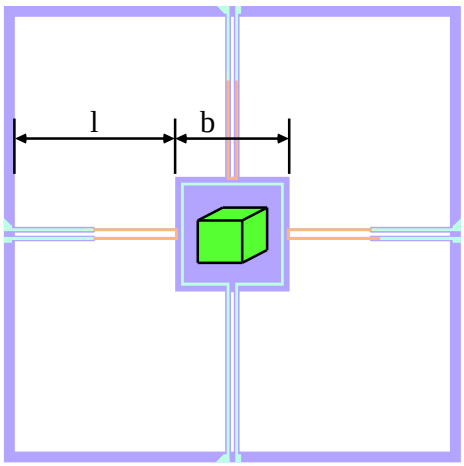

Figure 12.11: *Comparison of the existing design described in [1; 2; 3] (left) and our new squared design (right) with a mounted sample (green cube). Both sensors feature a metallic loop for calibration purposes. Piezoresistive parts are marked orange, the blue paths denote metallic conductors. The sensitivity depends on the ratio l/b.*

[1] C. Rossel *et al.*, J. Appl. Phys. **79** (11), 8166 (1996).
[2] M. Willemin *et al.*, J. Appl. Phys. **83** (3), 1163 (1998).
[3] C. Rossel *et al.*, Rev. Sci. Instrum. **69** (9), 3203 (1998).

12.4.2 Developments of LEμSR and the new μE4 surface muon beam

In the year 2002 the construction of the new surface muon beam line for LEμSR at the Paul Scherrer Institute (PSI) entered the phase of detail work with construction and manufacturing of the mechan-

ical elements, detailed specification and purchase order of the magnetic quadrupoles, dipoles and solenoids of the corresponding power supplies and design of the new area layout including shielding and support infrastructure. The main motivation for this beam is to increase the intensity of low energy muons, which is directly proportional to the flux of incoming surface muons over a 30×30 mm^2 area.

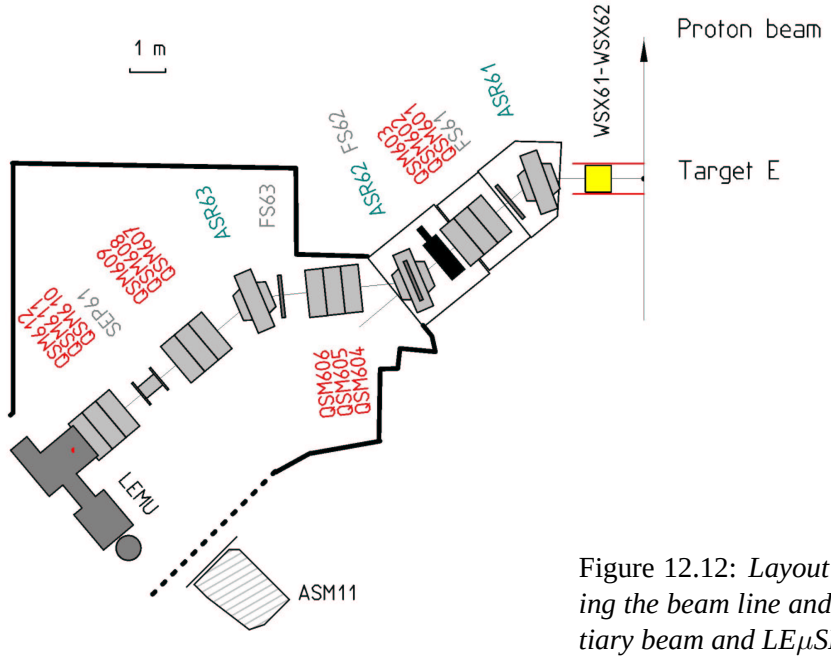

Figure 12.12: *Layout of the new μE4 area, showing the beam line and the position of the LEM tertiary beam and LEμSR spectrometer (LEMU).*

Furthermore, we started detailed work to upgrade the LEμSR apparatus. The main purpose of it is twofold. Firstly, an adaptation to the different beam conditions (larger phase space and intensity with respect to the presently used πE3). The second goal is to improve the operation and reliability of this delicate apparatus in view of an increasing number of experiments and users in the future. The first condition requires a new moderator and injection chamber with large acceptance, which have been designed and the construction of a segmented fast muon counter able to cope with rates in excess of 10^8 cps.

In order to comply with the semi-dedicated character of the new beam line a major mechanical rebuild of the entire apparatus has been initiated. The LEμSR apparatus (tertiary beam line and μSR spectrometer) will be rebuilt on a new single multipurpose platform, which will allow to move the LEμSR apparatus in and out of the area in a reasonable time.